TÜRKİYE 9. PETROL KONGRESİ
TMMOB JEOFİZİK MÜHENDİSLERİ ODASI
TÜRKİYE PETROL JEOLOGLARI DERNEĞİ
TMMOB PETROL MÜHENDİSLERİ ODASI

TARİH (DATE): 17-21, 2 ,1992

9th PETROLEUM CONGRESS OF TÜRKİYE
UCTEA CHAMBER OF GEOPHYSICAL ENGINEERS
TURKISH ASSOCIATION OF PETROLEUM GEOLOGIST
UCTEA CHAMBER OF PETROLEUM ENGINEERS

YER (PLACE): HILTON-ANKARA

RADON TRANSFORM

RADON DÖNÜŞÜMÜ

NECATİ GÜLÜNAY, HALLIBURTON GEOPHYSICAL SERVICES, SUGAR LAND, TX.

ÖZET

Rezidüel düzeltme (RNMO) ve toplama işlemine dayanan parabolic Radon dönüşümü lineer düzeltme (LMO) ve toplam işlemine dayanan lineer Radon dönüşümüyle yakından ilgilidir. Her iki işlem de f-x bölgesinde uygulanabilir. Bu bölgede RNMO, üssü uzaklığın karesiyle orantılı karmaşık sayılardan oluşurken LMO üssü uzaklığın kendisiyle orantılı karmaşık sayılardan oluşur. Verilmiş her bir frekans için dönüşüm katsayıları, uzaklık üzerinden toplam yapmak yerine en küçük kareler yöntemi kullanılarak elde edilirse eldeki kayıdın içerdiği lineer ya da parabolik eğimli bilgiye en iyi şekilde uyan bir model elde edilebilir. Bu tekniklerden RNMO kullananına *Radon tau-p* ve LMO kullanına *Radon tau-q* adını verilebiliriz. Bu teknikler kayıtlardaki tekrar eden bilgilerin (multiple) yok edilmesinde ve düzenli ya da düzensiz gürültünün giderilmesinde kullanılabilirler. Ancak, tekniklerin etkinliği olayların dönüşüm sırasında ne kadar iyi ayırt edilebildiklerine bağlıdır. Bu makale Radon dönüşümünün ayırma gücünü incelemektedir.

Eldeki problemin belirsiz (singüler) olmadığı durumlarda Radon tau-p ve Radon tau-q işlemleri eldeki matrisin tersi alınırken küçük miktarlarda beyaz gürültü kullanabildiklerinden, bu hallerde bu işlemlerin ayırma güçleri klasik tau-p (lineer düzeltme ve toplam) ve klasik tau-q (RNMO ve toplam) işlemlerinin ayırma güçlerinden üstündür. Klasik tau-q işleminin *sidelob*ları Fresnel integralleriyle yakından ilgili olup büyüklükleri azımsanamıyacak kadar yüksektir. Radon dönüşümü belirsizlik (singularity) durumlarında bile bu sidelobları etkin bir şekilde bastırmaktadir. Bu nedenle Radon tau-q işleminden geçmiş kayıtlar klasik tau-q işleminden geçmiş (normal toplam) kayıtlardan daha temizdirler.

ABSTRACT

The parabolic Radon transform based on residual normal moveout(RNMO) and stack is comparable to the linear Radon transform which is based on linear moveout(LMO) and stack. Both of these processes can be implemented in the f-x domain. In this domain, RNMO involves complex exponentials with arguments which are quadratic in offset while LMO involves arguments which are linear in offset. When the coefficients of the transforms at each frequency are obtained through a least squares error constraint rather than through straight summation in the frequency domain, a best fit is obtained to the dips or the residual moveout existing in the data. We will use the term *Radon τ-q* for the one which involves RNMO and the term *Radon τ-p* for the which involves LMO. Multiple elimination and/or coherent as well as random noise suppression can be achieved using either one of these Radon transforms. However, the effectiveness of the processes depend on how well the events are resolved in the forward domain. This paper studies the resolution of the Radon transforms. The resolution of either of the Radon τ-p or the Radon τ-q is better than that of the classical τ-p (slant stack) or the classical τ-q (RNMO and stack) *only* when the problem at hand is *non-singular* to allow the amount of white noise used in the matrix inversion to be small. The side lobes of the classical RNMO and stack are related to the Fresnel Integrals and are significant in magnitude. The least squares error nature of the Radon τ-q suppresses these side lobes significantly, even in *singular* cases. Therefore, the Radon τ-q gathers are always cleaner than those of the classical τ-q.

RADON TRANSFORM

RADON DÖNÜŞÜMÜ

INTRODUCTION

The classical τ-p method is well established (Phinney et al.,1981 and Tatham,1984). In simple terms, it is the modeling (inversion) of data in terms of assumed number of linear events (p values). The forward transform is achieved by performing linear moveout and then stack (slant stack) in the t-x domain. A convolutional operator known as the *Rho filter*, which is equivalent to a linear ramp in the frequency domain balances the spectrum of the forward transform. A common application of τ-p transform is to manipulate the forward transform, such as muting undesired dips, and then doing the inverse transform. The inverse transform is also performed using linear moveout.

Thorson(1984) imposed the least squares error constraint on the reconstructed data and developed *Slant Stack Stochastic Inversion*. He also generalized stacking velocity decomposition into *Velocity Stack Stochastic Inversion*. Hampson(1986) was able to implement Thorson's method efficiently by using NMO corrected data, the parabolic approximation to residual moveout, and the f-x domain.

Hampson's technique imposes the least squares error constraint on the model constructed for the data at each frequency. Hampson(1987) identified his approach as the Discrete Radon Transform which is explored by Beyklin (1987). Yilmaz(1989) extended Hampson's technique to pre NMO data by eliminating NMO application through the use of t-t^2 transform.

Seeing the success of Hampson's technique in suppressing noise on prestack gathers we have developed its linear version (Radon τ-p) and used it for noise elimination. During the development we have assumed that the Radon τ-p should be better than the classical τ-p because of the least squares approach. This paper is the result of questioning that assumption, and another which is counterpart to it: *Is Hampson's method really better than the residual moveout and stack?*. These questions led to the observation that the classical results are obtained from the least squares techniques when a large amount of white noise is used in the complex Wiener-Levinson algorithm and this in a sense unifies these methods.

In what we call the *Radon τ-p*, we use parameter p for linear moveout

$$t=\tau+px \qquad (linear\ move\text{-}out) \tag{1}$$

and therefore refer to Hampson's method as the *Radon τ-q* where q is the parameter for residual (parabolic) moveout

$$t=\tau+qx^2 \qquad (residual\ move\text{-}out) \tag{2}$$

In the Radon τ-p method the slant stack inverse in the f-x domain is found using an approach parallel to Hampson's *Inverse velocity stack*. The base functions in the Radon τ-p are $e^{j\,2\pi\,f\,p\,x}$ instead of $e^{j\,2\pi\,f\,q\,x\,x}$. Because of its least square nature the Radon τ-p might be referred to as the *F-x domain least squares τ-p*.

THE SLANT STACK IN THE F-X DOMAIN

Most time domain implementations of the τ-p transform require interpolation of the data from discrete time samples to the time values implied by Eq. 1. In the forward transform, linear moveout is applied by the amount -p.x and the results are summed. Division by number of elements normalizes the summation. Since a time shift is a linear phase shift to the data in the frequency domain, the frequency response of the τ-p trace at frequency f will be

$$c(f,p)=\frac{1}{N_x}\sum_{k=1}^{N_x} D(f,x_k)e^{-j2\pi fpx_k} \tag{3}$$

where N_x is the number traces in the data, x_k are the offsets, and $D(f,x_k)$ is the Fourier transform sample; kth trace, frequency f. The inverse Fourier transform of c(f , p) is the slant stack trace or the τ-p trace. Note that there is no *Rho filter* in the classical τ-p trace as defined here.

The resolution of the classical τ-p process can be studied as a function of frequency if we use a flat event at time t_0 :

$$c(f,p) = e^{j2\pi ft_0}\ a(f,p) \tag{4}$$

where

$$a(f,p) = \frac{1}{N_x}\sum_{k=1}^{N_x} e^{-j2\pi fpx_k} \tag{5}$$

Note that the sign convention followed throughout this paper is to use a plus sign for the exponent in the forward Fourier transform and a minus sign in the inverse Fourier transform. Therefore the Fourier transform of a spike at time t_0 is $e^{j\,2\pi f\,t0}$.

If the trace offset increment is a constant (δx), then the sum in Eq. 5 becomes the sum for a power series. And its sum is equal to

$$c(f,p)=\frac{1}{N_x}\frac{|\sin(\pi f N_x p\delta x)|}{|\sin(\pi f p\delta x)|}=\frac{1}{N_x}\frac{|\sin\pi f N_x\delta t)|}{|\sin(\pi f\delta t)|}=\frac{\delta x}{X_{max}}\frac{|\sin(\pi f p X_{max})|}{|\sin(\pi f p\,\delta x)|} \qquad (6)$$

as long as the value of fp δx is not equal to an integer

$f_a p_a \delta x_a = f_a \delta t_a = 0,1,2 \ldots$.

where subscript *a* stands for *alias* and $\delta t = p\,\delta x$ is the dip per trace, and $X_{max} = N_x \delta x$ is the spread length. At such values of f_a , p_a and δx_a the value of the sum is exactly equal to one:

$$c(f,p) = 1$$

The function given in Eq. 6 occurs in many branches of science. For example, the magnitude of diffracted light from a grating of N_x elements with element width δx is given by the same formula where δt is a parameter related to the angle measured from the direction of the incident light beam. The same equation is also used in seismic data acquisition in finding the response of a seismometer array to an incoming plane wave (Graebner 1960, Holzman 1963).

If viewed as a function p or δt, the function in Eq. 6 determines the resolution of the process. To find the half power point of the response involves trigonometric equations. Instead, the first zero crossing value given by

$$\delta T = N_x\,\delta t = \frac{1}{f} \qquad (7)$$

can be used.

Note that δT is the linear moveout at the far offset.

The plot of Eq. 6 as a function of frequency is given in Figure 1a for three dips : dT = 0 , dT = 10 ms and dT = 20ms and for a 12 trace flat event with zero dip. The trace spacing is 500 ft and the maximum offset is 6000 ft. Figure 1b is a similar plot for dT = 50 ms and points to the aliasing at 240 Hz.

The plot of Eq. 6 as a function of δT at 15 Hz is given in Figure 3. The first zero crossing occurs at 67 ms. Two dipping events with far offset linear moveout difference less than this amount are considered to be unresolvable. This is known as *Rayleigh's Criterion* in Optics (Born and Wolf,1980).

THE RADON τ-p

The Fourier transform of a record with a single event at intercept time t_0 and slope p is $e^{j2\pi f\,t0}$ $e^{j2\pi f\,p\,x}$. Therefore we model the dip and offset dependent variations in the input data in terms of base functions $e^{j2\pi f\,p\,x}$. When the least squares error condition is used for f-x domain τ-p, we require that the model coefficients to fit the data in the least squares sense at each frequency:

$$\sum_{k=1}^{N_x}\left|D(f,x_k)-\sum_{i=1}^{N_p}s(f,p_i)e^{j2\pi fp_ix_k}\right|^2=minimum \qquad (8)$$

Then a system of normal equations is obtained at each frequency for N_p unknown (model) coefficients $s_n = s(f,p_n)$ $(n = 1,,..,N_p)$,

$$\sum_{n=1}^{N_p} R_{mn}\, s_n = g_m \qquad (9)$$

$$Rs = g$$

where N_p is the number of dips the data are assumed to contain and

$$g_m = g(f,p_m) = \frac{1}{N_x}\sum_{k=1}^{N_x} D(f,x_k)e^{-j2\pi f p_m x_k} \qquad (10)$$

$$R_{mn} = R(f,p_m,p_n) = \frac{1}{N_x}\sum_{k=1}^{N_x} e^{j2\pi f(p_n-p_m)x_k} \qquad (11)$$

We are modeling (inverting) the data in terms of N_p dipping events with p values ranging from p_1 to p_{Np}.

An important observation is that the right hand side of Eq. 9 (given by Eq.10) is the classical τ-p response defined by Eq.3

$$g(f,p_i) = c(f,p_i) \; . \qquad (12)$$

The **R** matrix on the left hand side is independent of the data, and its inverse is like a deconvolution operator for the solution:

$$s = R^{-1}\, c \qquad (13)$$

$\mathbf{R^{-1}}$ operating on the classical τ-p response deconvolves the effects of finite apertures resulting with highly resolved output in p direction.

When the dip increment at a particular frequency is chosen to be constant and is δp, the matrix becomes Hermitian Toeplitz (Kostov, 1989). Then, the main diagonal is all ones and the nth lower diagonal is given by

$$R_n = \frac{1}{N_x}\sum_{k=1}^{N_x} e^{-j2\pi f n(\delta p)x_k} \; . \qquad (14)$$

Then, the linear system of equations given in Eq. 9 can be efficiently solved and it is computationally feasible to use large N_p values in modeling the data if necessary.

Important observations are:

a). R_n diminishes in magnitude as the spread length $X_{max} = N_x * \delta x$ increases. When X_{max} goes to infinity the **R** matrix reduces to a unit matrix unless aliasing occurs. When aliasing occurs, the **R** matrix becomes singular and can not be inverted unless a large amount of white noise is injected to its main diagonal. We will see in the next section that when white noise is large, the Radon τ-p and the classical τ-p results agree. Therefore, the infinite aperture limit of the Radon τ-p is equivalent to the classical τ-p.

b). R_n array is the same as the **c** array of the flat event given by Eq. 5. Therefore Eq. 9 has to return a perfect solution (a spike) for the **s** array. That is, the Radon τ-p can produce the ideal model, *the infinite aperture solution*, from finite apertures if the matrix to be inverted is non-singular.

EFFECTS OF WHITE NOISE ON THE RADON τ-p

Various conditions cause the **R** matrix to be singular (Kostov, 1989). Aliased frequencies (or p ranges) have already been mentioned in the previous section. The case of frequencies around zero Hz is a good example of the numerical problems singularities cause. At zero Hz the matrix becomes all ones and is impossible to invert. To decrease the arithmetic problems caused by such singularities, it is common to add some white noise to the main diagonal of the **R** matrix, changing it from $R_0 = 1$ to $R_0 = 1+n$ where n is a small positive value. To eliminate the amplitude loss this modification will cause on the solution array **s**, the right hand side of Eq. 9 can be multiplied by $1+n$. This is equivalent to keeping the main diagonal of **R** equal to 1 but dividing all other diagonals by $1+n$. With this scheme an algorithm can be obtained which gives **s** = **c** as white noise parameter *n* goes to infinity. Therefore the Radon τ-p reduces to the classical τ-p as the added white noise goes to infinity.

Because of cost considerations the matrix inversion is usually attempted without calculating the determinant of the matrix being inverted. Therefore the usual practice is to inject a small and user given white noise whether the matrix is singular or not. When the matrix is not singular and the white noise happens to be small, then this is the best solution (in the least square sense) that can be constructed from the assumed dips. On the other hand, if the value of white noise is small and the

case is singular, then the solution at that frequency is unreliable. Since a diagonal which is not a main diagonal and has a magnitude equal to one gives singularity, some of the singularities can be eliminated by varying the noise parameter as a function of $|R_m|$ where m is the index of the non-main-diagonal which has the largest magnitude.

To understand the effect of white noise on the Radon τ-p(or τ-q) solution we used the same record that contains a flat event at time t and model it in terms of two dips: one is the correct dip ($dip_1 = 0$) the other one is an incorrect one ($dip_2 = dt$). The normal equations become

$$\begin{pmatrix} 1+n & a^* \\ a & 1+n \end{pmatrix} \begin{pmatrix} s_1 \\ s_2 \end{pmatrix} = e^{j2\pi f t_0}(1+n) \begin{pmatrix} 1 \\ a \end{pmatrix} \qquad (15)$$

where a is given by Eq. 5 and a^* is its complex conjugate.

The determinant of the matrix is

$$D = (1+n)^2 - a^* a \qquad (16)$$

and the analytical solution for the Radon τ-p can be shown to be

$$\begin{pmatrix} s_1 \\ s_2 \end{pmatrix} = \frac{e^{j2\pi f t_0}}{D} \begin{pmatrix} (1+n)^2 - (1+n)a^* a \\ (1+n)na \end{pmatrix} \qquad (17)$$

We made three observations from this simple case:
a). As the white noise parameter goes to infinity, we obtain the expected classical τ-p solution

$$\begin{pmatrix} s_1 \\ s_2 \end{pmatrix} = e^{j2\pi f t_0} \begin{pmatrix} 1 \\ a \end{pmatrix} \qquad (18)$$

b). As the white noise parameter goes to zero, we obtain the ideal solution

$$\begin{pmatrix} s_1 \\ s_2 \end{pmatrix} = e^{j2\pi f t_0} \begin{pmatrix} 1 \\ 0 \end{pmatrix} . \qquad (19)$$

For N_p dips we would get

$$\begin{pmatrix} s_1 \\ s_2 \\ . \\ . \\ . \\ s_{N_p} \end{pmatrix} = e^{j2\pi f t_0} \begin{pmatrix} 1 \\ 0 \\ 0 \\ . \\ . \\ . \\ 0 \end{pmatrix} \qquad (20)$$

That is, no energy leaks from the correct dip (dip = 0) to the incorrect ones when a zero value can be used for the white noise parameter.

c). At zero Hz, $a^* . a = 1$, and we obtain

$$s_1 = s_2 = e^{j2\pi f t_0} \frac{1+n}{2+n} . \qquad (21)$$

It can be shown that at zero Hz, for N_p dips we get

$$s_1 = s_2 = \ldots = s_{N_p} = e^{j2\pi f t_0} \frac{1+n}{N_p+n} . \qquad (22)$$

This means that it is not possible to determine to what dip DC energy belongs and therefore the Radon τ-p distributes that energy equally between all dips.

The spectra of the Radon τ-p traces when Np = 2 and for the record used above is given in Figures 2a through 2f for various white noise levels. Two dips , dT = 0 and dT = 10ms at X_{max} = 6000 ft are used in modeling the data. We observe the following
a). energy around zero Hz is equally shared between both dips,
b). as the white noise percent goes to zero the trace with dT = 10 ms looses its energy to the trace dT = 0,
c). as the white noise increases(Figure 2a) the same

solution as the classical tau-p is obtained(Figure 1a)

Figure 4 illustrates similar points using 7 dips to model this data instead of 2, and compares the results to that of the classical τ-p. The dip increment used is 36 ms at the far offset. Note the resolution increase when the white noise is small. Also note that the true amplitude nature of Radon τ-p is lost as the amount of injected white noise increases. In the very high noise limit (10000 %) we obtained the classical τ-p result. The classical τ-p is not a true amplitude process since it produces energy at the dips where data does not contain any energy.

Using 41 dips given in Figure 3 for the Radon τ-p results with a singularity since the number of unknowns ($N_p = 41$) is larger than the number of equations ($N_x = 12$) in the problem. We observed that using a moderate white noise level such as 1 % eliminates most of the numerical the problems such singularities cause, but the results are no different from those of the classical τ-p.

For the synthetic record used above the spectrum of the forward transform trace for $p = 0$ is flat for the classical τ-p (Figure 1a). The *Rho-filter* which is a multiplication of the spectrum by frequency (i.e. a linear ramp) is later imposed on the classical forward τ-p transform (Tatham,1984). The $p = 0$ trace of the Radon τ-p shares some of its energy with other p traces when the injected white noise is nonzero as described by Eq.22 and as observed above. We find that as the number of dips used to model the input data goes to infinity, the amplitude spectrum of the $p = 0$ trace of these synthetics becomes a line implying that Radon τ-p approaches to the Rho filtered τ-p as the number of dips used to model the data (Np) becomes very large.

THE RESIDUAL MOVEOUT AND STACK IN THE F-X DOMAIN

The residual moveout after NMO, followed by stack can be done through the f-x domain parallel to Eq.3:

$$c(f,q) = \frac{1}{N_x}\sum_{k=1}^{N_x} D(f,x_k)e^{-j2\pi f q x_k^2} \qquad (23)$$

where D(f, x_k) represent the Fourier transform of the NMO applied data at offset x_k and q is the residual move-out parameter. q can be calculated using

$$q = \left(\frac{1}{V_e^2} - \frac{1}{V_{nmo}^2}\right)\frac{1}{2t_0} \qquad (24)$$

where V_e is the velocity of the hyperbolic event, V_{nmo} is the NMO velocity, and t_0 is the zero offset time of the event. The inverse Fourier transform of c(f , q) is the RNMO + stack trace (the τ-q trace).

The resolution of the τ-q trace can be studied as a function of frequency or moveout using the same flat event as used previously. The flat event has $q = 0$. Then

$$c(f,q) = e^{j2\pi f t_0}\, b(f,q) \qquad (25)$$

where

$$b(f,q) = \frac{1}{N_x}\sum_{k=1}^{N_x} e^{-j2\pi f q x_k^2} \qquad (26)$$

This sum behaves like the Fresnel Integrals

$$\int_0^V \cos(\pi\frac{U^2}{2})dU$$

$$\int_0^V \sin(\pi\frac{U^2}{2})dU$$

which are both used in optics for the diffraction of light from a straight edge(Born & Wolf, 1980). In this application
where

$$V = (N_h - 1)dU \tag{27}$$

$$dU = 2\,\delta x\,\sqrt{fq} \tag{28}$$

and $N_h = N_x$ for offend shooting and $N_h = N_x/2$ for split spread. Since each of the Fresnel integrals oscillate around the limit value of 0.5 as V goes to infinity, the sum in Eq. 26 has a frequency and moveout dependent limit:

$$\frac{0.5|1+j|}{2N_x\,\delta x\,\sqrt{fq}} = \frac{0.353}{\sqrt{f\,\delta T}} \tag{29}$$

where δT is the residual moveout at far offset:

$$\delta T = q\,(N_x\,\delta x)^2 = q\,X_{max}^2 \tag{30}$$

The plot of Eq. 26 at 15 Hz and as a function of δT is shown in Figure 5. Note the significant side lobes in the figure. Only at high frequencies or at moveouts that differ from that of the event or for large spatial apertures will the bias in the oscillation point be small. Otherwise, the classical τ-q will exhibit significant side lobes, which explains why a single event shows up on many velocity panels in standard CVS panels.

THE RADON τ-q

When the least squares error constraint is imposed on the f-x domain τ-q at each frequency, we obtain Hampson's method(1986) which we call *Radon* τ-q.

When the q increment (δq) is kept constant, a set of normal equations with Hermitian Toeplitz form are obtained as before. The only difference is that δq takes the place of the parameter δp and x^2 takes the place of x:

$$\sum_{n=1}^{N_q} R_{mn}\,s_n = g_m \tag{31a}$$

$$Rs = g$$

where N_q is the number of q values the data is assumed to contain and

$$g_m = g(f,q_m) = \frac{1}{N_x}\sum_{k=1}^{N_x} D(f,x_k)e^{-f2\pi f q_m x_k^2} \tag{31b}$$

and

$$R_{mn} = R(f,q_m,q_n) = \frac{1}{N_x}\sum_{k=1}^{N_x} e^{f2\pi f(q_n-q_m)x_k^2} \tag{31c}$$

The diagonals of the **R** matrix in the parabolic case are

$$R_n = \frac{1}{N_x}\sum_{k=1}^{N_x} e^{-f2\pi f n(\delta q)x_k^2} \tag{32}$$

I again make the observation that the right hand side of the normal equations given above is the classical τ-q transform:

$$g(f,q_i) = c(f,q_i) \tag{33}$$

Similar considerations to the ones in τ-p lead to the following conclusions:

a. The large aperture limit of the Radon τ-q is the classical τ-q.
b. The high white noise limit of the Radon τ-q is the classical τ-q.
c. The energy at zero Hz is equally shared between all curvatures and therefore that value goes to zero as the number of parabolas used in the model goes to infinity.

Figure 6 compares the Radon τ-q to the classical τ-q using five different white noise values. Note the resolution increase and the side lobe suppression in Radon τ-q when the white noise used is small. When the matrix is singular a moderate noise value needs to be used. Even in singularity cases side lobe suppression takes place in Radon τ-q, though the resolution is no different from the classical τ-q.

CONCLUSIONS

The least squares τ-p and the least squares τ-q can be implemented in the f-x domain in similar fashions. The infinite aperture or infinite white noise limit of both processes yields classical counterparts, the slant stack, and the residual moveout and stack. When the matrices to be inverted are non-singular, both methods eliminate the smearing effect that finite apertures cause, giving highly resolved (infinite aperture type) results. When matrices are singular large white noise values must be used. In such cases Radon τ-p produces a result which is almost identical to the classical τ-p. The Radon τ-q, when used with such white noise levels suppresses the side lobes observed in the classical residual move-out and stack, yet does not sharpen the main lobe, and therefore has the same resolution as the classical residual moveout and stack.

ACKNOWLEDGMENTS

I thank Cam Wason for many discussions, especially on the resolution issue. I am also grateful to Halliburton Geophysical Services for allowing me to present this work.

REFERENCES

Beyklin, G. (1987), Discrete Radon Transform, IEEE Transactions on Acoustics, Speech and Signal Processing Proceedings, Vol. ASSP-35, No. 2, Feb. 1987, pp. 162-172.

Born, M., Wolf, E. (1980), Principles of Optics, Pergamon Press.

Graebner, R. J. (1960), Seismic data enhancement, A case history, Geophysics, Vol.25, No.1 pp.283-311.

Hampson, D. (1986) Inverse velocity stacking for multiple elimination Journal of the Canadian Society of Exploration Geophysicists, Vol.22, No.1, December, p. 44-55

Hampson, D.(1987) The discrete Radon transform: A new tool for image enhancement and noise suppression. Presented in the 57th Annual International Meeting of the Society of Exploration Geophysicists in New Orleans, Expanded Abstract p. 141.

Holzman, M.(1963) , Chebyshev optimized geophone arrays, Geophysics, Vol.28, No. 2, p.145.
Kostov, C.(1989), Finite-aperture slant-stack transforms, SEP-61, page 261.

Naponen, I., and Keeney, J., 1983, Attenuation of water born coherent noise by application of hyperbolic velocity filtering during tau-p transform: Presented at the 53rd Annual International SEG meeting, September 12, in Las Vegas.

Phinney, R.A., Chowdhury, K.R., and Frazer, L.N. (1981), Transformation and analysis of record sections,Journal of Geophysical Research, Vol. 86, No. 1, pp. 359-377, Jan.10,1981.

Tatham,R.H., Keeney,J.W., and Naponen,I.(1982) Application of the τ-p transform (Slant Stack) in processing seismic data, Presented in the 52nd Annual International meeting of the Society of Exploration Geophysicists in Dallas, TX.

Tatham, R.H. (1984) Multidimensional Filtering of Seismic data, Proceedings of the IEEE, Vol. 72, No.10, pp.1357-1369, Oct.1984.

Thorson, J.R.,(1984) Velocity Stack and Slant Stack inversion methods. Ph.D thesis, Stanford University, May 1984.

Yilmaz, O.(1989) Velocity-Stack Processing, Geophysical Prospecting, Vol.37, p.357-382

RADON TRANSFORM

RADON DÖNÜŞÜMÜ

Figure 1a: Spectra of the classical tau-p traces for 12 trace flat event

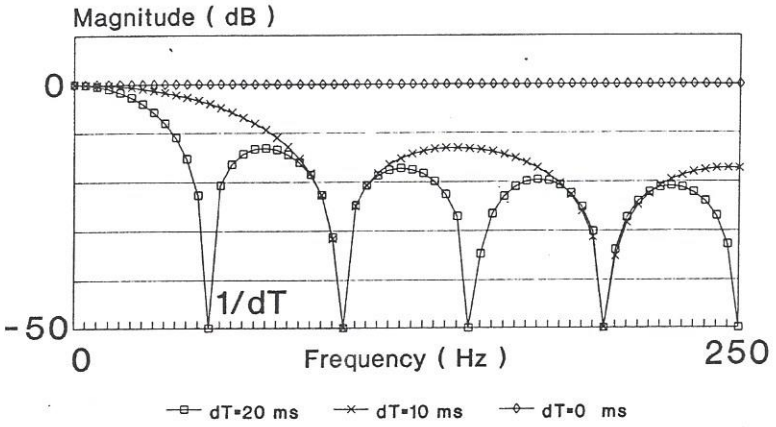

dx:500, Nx:12, Xmax=6000, dT=p.Xmax

Figure 1b: Spectrum of a classical tau-p trace for 12 trace flat event

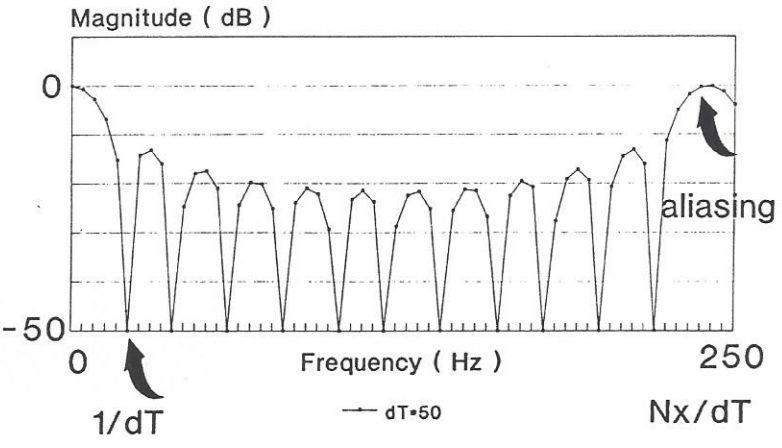

dx:500, Nx:12, Xmax=6000, dT=p.Xmax

RADON TRANSFORM

RADON DÖNÜŞÜMÜ

Figure 2a: Spectra of the Radon tau-p traces at Noise=10000 %

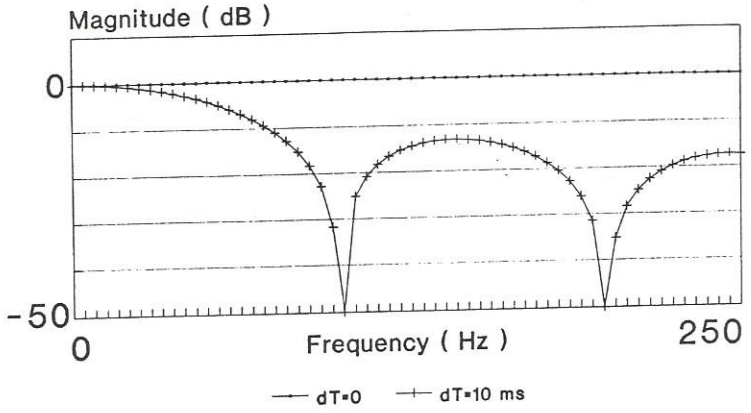

dx=500 Nx=12 Xmax=6000 dT=p.Xmax Np=2

Figure 2b: Spectra of the Radon tau-p traces at Noise=100 %

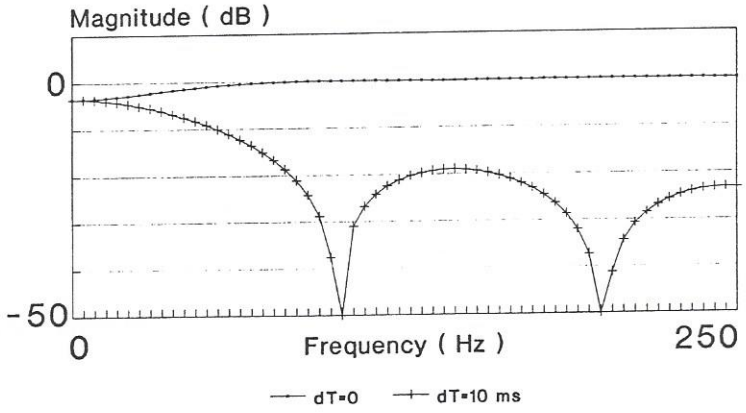

dx=500 Nx=12 Xmax=6000 dT=p.Xmax Np=2

Figure 2c: Spectra of the Radon tau-p traces at Noise=10 %

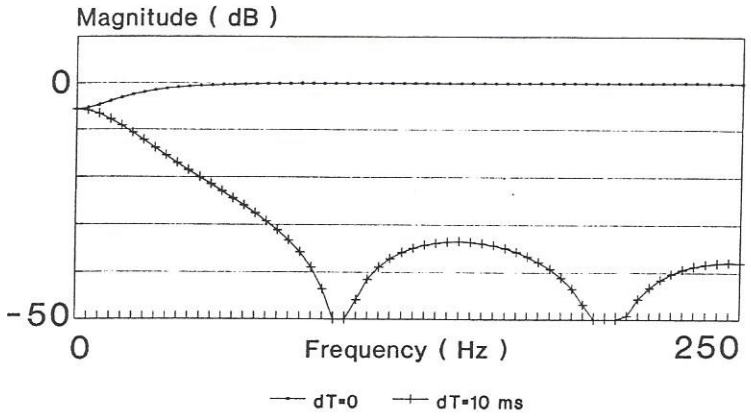

dx=500 Nx=12 Xmax=6000 dT=p.Xmax Np=2

Figure 2d: Spectra of the Radon tau-p traces at Noise=1 %

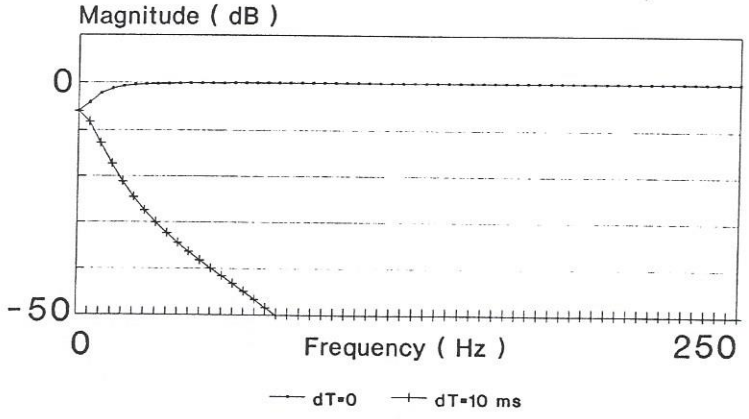

dx=500 Nx=12 Xmax=6000 dT=p.Xmax Np=2

RADON TRANSFORM

RADON DÖNÜŞÜMÜ

Figure 2e: Spectra of the Radon tau-p traces at Noise=0.1 %

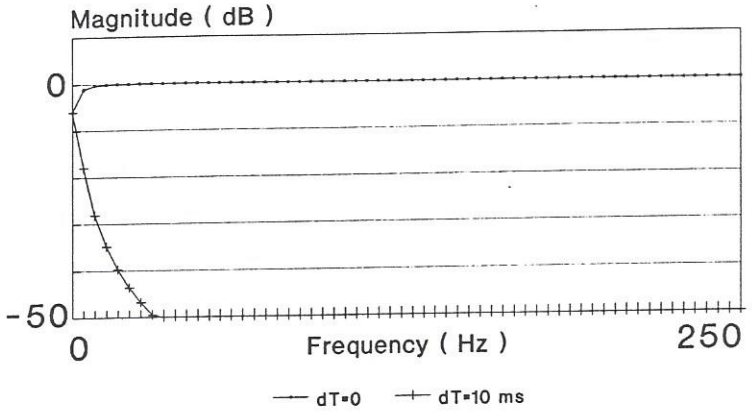

dx=500 Nx=12 Xmax=6000 dT=p.Xmax Np=2

Figure 2f: Spectra of the Radon tau-p traces at Noise=0.01 %

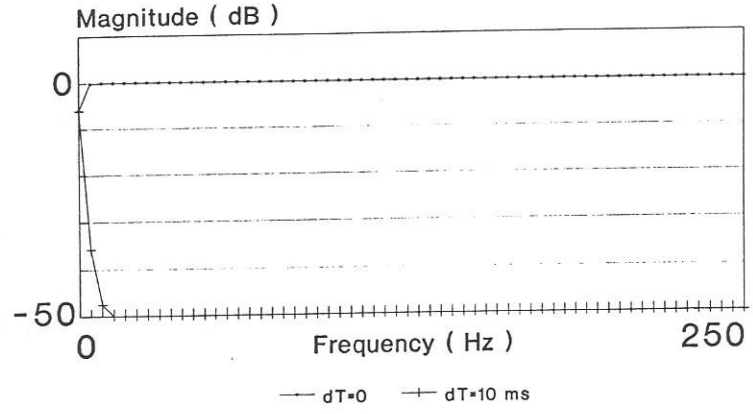

dx=500 Nx=12 Xmax=6000 dT=p.Xmax Np=2

RADON TRANSFORM

RADON DÖNÜŞÜMÜ

Figure 3: Classical tau-p response at 15 Hz.

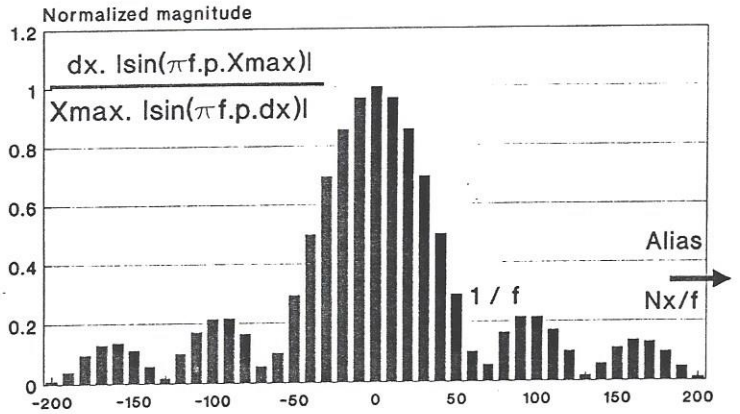

dx:500 ft, Nx:12, f:15 Hz, Xmax=6000 ft

Np=41

Figure 4: Radon tau-p response at 15 Hz.

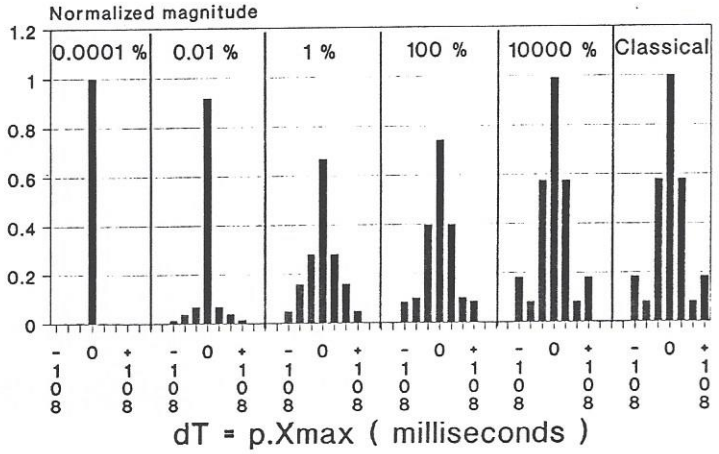

dx=500 ft, Nx=12, Xmax=6000 ft, Np=7

RADON TRANSFORM

RADON DÖNÜŞÜMÜ

Figure 5: Classical tau-q response at 15 Hz.

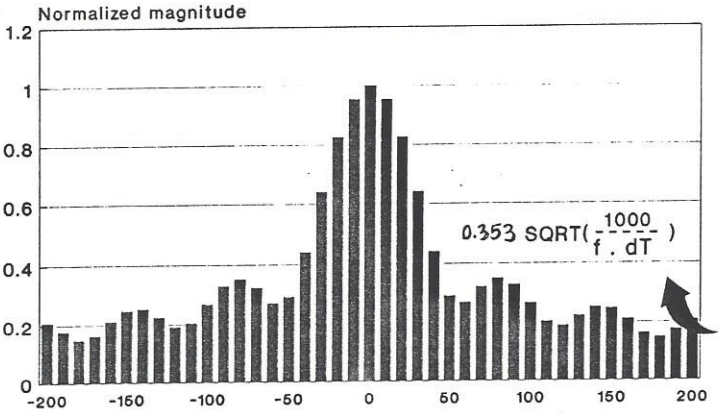

Figure 6: Radon tau-q response at 15 Hz.